Breast Cancer: Targets and Therapy

Dovepress
open access to scientific and medical research

Open Access Full Text Article

ORIGINAL RESEARCH

Internalization: acute apoptosis of breast cancer cells using herceptin-immobilized gold nanoparticles

This article was published in the following Dove Press journal:
Breast Cancer: Targets and Therapy
10 February 2015
Number of times this article has been viewed

Pierson Rathinaraj[1]
Ahmed M Al-Jumaily[1]
Do Sung Huh[2]

[1]Institute of Biomedical Technologies, Auckland University of Technology, Auckland, New Zealand; [2]Department of Nano science and Engineering, Inje University, Gimhea, South Korea

Abstract: Herceptin, the monoclonal antibody, was successfully immobilized on gold nanoparticles (GNPs) to improve their precise interactions with breast cancer cells (SK-BR3). The mean size of the GNPs (29 nm), as determined by dynamic light scattering, enlarged to 82 nm after herceptin immobilization. The in vitro cell culture experiment indicated that human skin cells (FB) proliferated well in the presence of herceptin-conjugated GNP (GNP–Her), while most of the breast cancer cells (SK-BR3) had died. To elucidate the mechanism of cell death, the interaction of breast cancer cells with GNP–Her was tracked by confocal laser scanning microscopy. Consequently, GNP–Her was found to be bound precisely to the membrane of the breast cancer cell, which became almost saturated after 6 hours incubation. This shows that the progression signal of SK-BR3 cells is retarded completely by the precise binding of antibody to the human epidermal growth factor receptor 2 receptor of the breast cancer cell membrane, causing cell death.

Keywords: herceptin, gold nanoparticles, SK-BR3 cells, intracellular uptake

Introduction

For more than a decade, nanometer-sized gold nanoparticles (GNPs) have attracted considerable attention not only because of their size- and shape-dependent optical and electronic properties but also due to their latent uses in thermal imaging, catalysis, scattering analysis, photoelectronic devices, biomedical diagnostics, and other related fields.[1–3] GNPs offer important new possibilities in cancer diagnosis and therapy[4] and can be used in the imaging[5,6] of tumors in their primary and secondary locations, as delivery agents for antitumor drugs, and for nonaggressive amputation treatments. The conveyance of the NPs to the tumor is a multistage technique.[7] Systemically controlled NPs with tumor-binding ligands can accumulate in the cancer cell due to the additional disordered vasculature relative to noncontaminated tissue.[6,7]

Cancer is challenging to treat, so active diagnosis approaches in the early phases of cancer are life threatening. In this respect, imaging has become an essential instrument in cancer medical trials and therapeutic replication.[8] Fluorescent bioimaging is also of extreme importance for visualizing the manifestation and movement of specific particles, cells, and biological processes that affect the performance of tumors and/or their reaction to therapeutic medications.[9] Therefore, an extensive series of fluorescent modules has been explored in in vitro bioimaging studies, including the biomarking of cancer tissues,[10] angiogenic vasculature, and sentry lymph nodes.[11] In this respect, numerous nanomaterials such as quantum dots, noble metal NPs, upconverted NPs, and new fusion nanocomposites of reduced graphene oxide and GNPs have great

Correspondence: Pierson Rathinaraj
Institute of Biomedical Technologies, Auckland University of Technology, WD 301, St Paul Street, Wellesley Campus, Auckland 1142, New Zealand
Tel +64 9 921 9999
Fax +64 9 921 9973
Email pierson.rathinaraj@aut.ac.nz

submit your manuscript | www.dovepress.com
Dovepress
http://dx.doi.org/10.2147/BCTT.S69834

potential for highly sensitive optical imaging of cancer in both in vitro and in vivo experiments. From this viewpoint, GNPs are innovative biocompatible nanoprobes, offering surfaces and cores that possess physicochemical properties (eg, optical chirality,[12,13] fluorescence,[14] near-infrared photoluminescence,[15] and ferromagnetism[16]) that offer novel openings for clinical diagnostics. As such, these tools will certainly play a vital part in the initial analysis and responsive recognition of tumors.

The multifunctional behavior of NPs offers exclusive benefits for the tumor-specific transfer of imaging and medicinal agents.[17] Monoclonal antibodies with substantially assorted structures and properties are economical to produce and have great feasibility as a class of tracking moieties.[18] One of the most broadly studied monoclonal antibodies used as a targeting moiety for the distribution of agents is herceptin. Herceptin is a water-soluble antibody that binds to the human epidermal growth factor receptor 2 (HER2) found on the membrane of SK-BR3 cells.

In this study, SK-BR3 cells were attacked with herceptin-conjugated GNPs (GNP–Her) for tumor treatment and diagnosis. Mercaptosuccinic acid (MSA)–immobilized GNPs were prepared by citrate reduction, followed by the coupling reaction of GNP with acid-terminated MSA. Herceptin was then immobilized on the surface of GNP (GNP–Her) to enrich the anticancer effects of chemotherapeutic agents.[19–22] The surface properties of GNP and GNP–Her were characterized by Fourier transform infrared (FT-IR) spectroscopy, ultraviolet–visible (UV–vis) spectrometry, dynamic light scattering (DLS), and transmission electron microscopy (TEM). To estimate the cell compatibility and cytotoxicity of the GNPs and GNP–Her conjugates, human breast cancer cells (SK-BR3) were cultured in the presence of GNPs. The intracellular uptake of GNP–Her into the cells was also observed by confocal laser scanning microscopy (CLSM) and inductively coupled plasma mass spectrometry (ICP–MS).[23]

Materials and methods

Auric chloride ($HAuCl_4$), sodium citrate ($Na_3C_6H_5O_7$), MSA, and herceptin were purchased from Hoffman-La Roche Ltd (Basel, Switzerland). Cell culture reagents, fetal bovine serum, Dulbecco's Modified Eagle's Medium (DMEM), penicillin–streptomycin mix, trypsin–ethylene diamine tetraacetic acid (EDTA) solution, Dulbecco's phosphate-buffered saline (PBS), and cell viability staining reagents were provided by Gibco BRL (Thermo Fisher Scientific, Waltham, MA, USA), and the cells (SK-BR3 and FB) were purchased from the Korean Cell Line Bank.

Synthesis of monodispersed GNPs

GNPs were prepared according to the method outlined by Anshup et al.[24] Briefly, in a 250 mL round-bottomed flask, 100 mL of 0.05% $HAuCl_4$ was added and heated. Under prompt stirring, 3.5 mL of sodium citrate (1%) was supplemented and further rapidly stirred for 15 minutes at 120°C. After 30 minutes of stirring, the solution was then steadily cooled to room temperature. The citrate concentration was adjusted to attain different particle sizes. After 15 minutes, the liquid was removed and cooled to room temperature and filtered. The prepared GNPs were resuspended and purified by centrifugation and double precipitation from distilled water.

Preparation of hydrophilic GNPs

MSA (0.16 M) was dissolved in 70 mL of water in a 250 mL three-necked flask containing GNPs. The solution was stirred for 3 hours in nitrogen atmosphere. After the reaction was complete, the water was separated by vacuum, and the residue was transferred into a centrifuge tube and mixed with 4 mL of water. Subsequently, 20 mL of water was added to the mixed solution, and the precipitated product was separated and subjected to centrifugation at 3,000 rpm (revolutions per minute) for 15 minutes and washed with water. The prepared MSA-conjugated GNPs were dissolved and purified by centrifugation and double precipitation from water.

Immobilization of herceptin on GNPs

The immobilization of herceptin on GNPs (GNP–Her) was carried out by the reaction of water-soluble GNPs with herceptin (Figure 1). Water-soluble GNPs (1.2 mmol) and herceptin

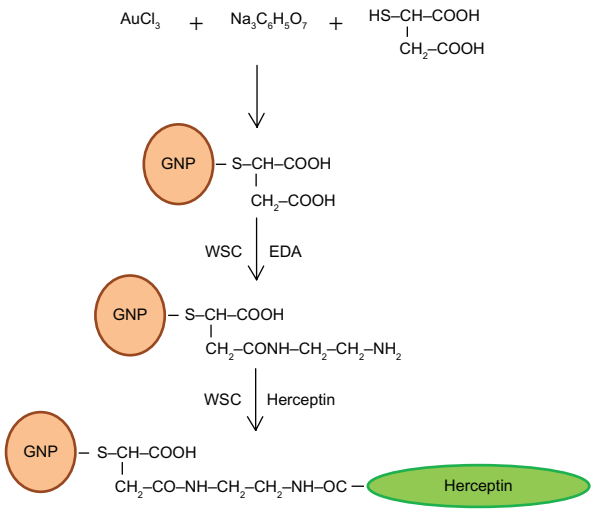

Figure 1 Schematic diagram showing the immobilization of herceptin on mercaptosuccinic acid-coated gold nanoparticles.
Abbreviations: EDA, ethylenediamine; GNP, gold nanoparticle; WSC, water-soluble carbodiimide.

(7 mmol) were added to a two-necked flask and dissolved in 10 mL of PBS buffer. 1-Ethyl-3-(3-dimethylaminopropyl) carbodiimide (EDC; 2 mmol) and *N*-hydroxysuccinimide (NHS; 2 mmol) were supplemented to the reaction solution, followed by stirring for nearly 5 hours at room temperature. The reaction product was filtered to remove the precipitate and added to a 100,000 molecular weight cutoff dialysis membrane in deionized water for 24 hours to discard the unreacted EDC, herceptin, and NHS. Lastly, the solution was filtered through a 0.45 μm membrane and dried under vacuum for 24 hours.

Preparation of cyanine dye–GNP–Her conjugates

Cyanine dye 5 (Cy5)-conjugated GNP–Her was obtained by reacting 1.5×10^{-3} mol/L GNP–Her with 4.8×10^{-5} mol/L fluorescent Cy5 in a carbonate buffer solution. The concentration of Cy5 dye was examined by UV–vis spectroscopy to calculate the number of NPs internalized into the cytoplasm of SK-BR3.[25]

Results

Characterization of surface-modified GNPs

The immobilization of herceptin and Cy5 dye on surface-modified GNPs was recorded by UV–vis absorption spectrum from aqueous solution at room temperature using a Hitachi U-3000 spectrophotometer. The core diameter and the surface morphology of GNPs were observed by TEM (Philips CM-200, 120 kV). The samples for TEM observations were diluted with distilled water and deposited on Formvar-coated 400-mesh copper grids. After drying the GNP–fluid thin film on the copper grid, a thin carbon film, approximately 10–30 nm in thickness, was deposited on the NP film. The size and hydrodynamic diameter distribution of the GNPs were determined by DLS using a light-scattering spectrometer BI90 (Brookhaven, Long Island, NY, USA).

Cell culture

SK-BR3 (breast cancer cells) was used as the target cell, and FB (human skin cells) was used as the control cell line. In a humidified atmosphere containing 5% CO_2, the cells were cultured routinely in a polystyrene dish at 37°C using 10 mL of McCoy medium or DMEM, supplemented with 10% fetal bovine serum and 1% penicillin–streptomycin G sodium. The medium was changed every 3 days. For subculture, the cells were washed twice with PBS and incubated with a trypsin–EDTA solution (0.25% trypsin, 1 mM EDTA) for 10 minutes at 37°C to detach the cells. Complete media were then added to the polystyrene dish at room temperature to prevent the effects of trypsin. The cells were washed thrice by centrifugation method and resuspended in a new culture dish. To observe the morphology of cells, the cells were seeded in a 10 mL Petri dish at a concentration of 1×10^5 cells/mL and incubated for 3 days with GNP and GNP–Her. The surface morphology of adhered cells was observed by Nikon Eclipse TS100 optical microscopy.

Cell viability

To study the cytotoxic effects of GNP–Her, after 3 days of culture, the SK-BR3 and FB cells were suspended in PBS at a density of 1×10^5 cells/mL. Subsequently, the cell suspension was mixed with 100 μL of the assay solution (10 μL propidium iodide–calcein AM) and incubated for 15 minutes at 37°C. The cells were then observed by fluorescence microscopy (Axioplan 2; Carl Zeiss Meditec AG, Jena, Germany) for the simultaneous observation of live and dead cells.

Intracellular uptake of GNPs

For the observation of effective cellular uptake of NPs via CLSM and fluorescence microscopy, the cells were seeded at a concentration of 1×10^5 cells/mL in a 10 mL culture dish and incubated for 24 hours. After 1 day, the medium was swapped with GNP and GNP–Her, containing a particle concentration of 50 μg/mL, and incubated for a certain period (2–7 hours) for the specific internalization of the NPs into the cells. The cells were then washed three times with PBS, and images were taken using a confocal laser microscope. A Carl Zeiss LSM 410 (Oberkochen, Germany) confocal laser scanning microscope was used to obtain the confocal images. The location and integrity of the internalized GNP–Her conjugates were estimated by CLSM using 4,6-diamidino-2-phenylindole dihydrochloride (DAPI, blue) as a marker, which stains the nuclei of the cells. The cell nuclei were stained by the addition of DAPI solution (10 μL) with proper mixing and incubated for 10 minutes. To track the GNP–Her NPs, GNP–Her and DAPI (488 nm) were added to the cells. The stained cells were washed at least three times with 1 mL of fresh DMEM and images were then taken by CLSM. To measure the intracellular uptake of the NPs, cells were grown in 24-well culture plates with roughly 10^5 cells in 1 mL of the medium. After 20 hours' incubation at 37°C, the cells were reseeded with culture medium containing GNP–Her at a concentration of 2×10^{-4} cells/mL. The intracellular gold concentration was quantified using ICP–MS. Cells were washed with PBS, separated, resuspended, counted,

and centrifuged, and the cell pellets were dissolved in 37% HCl aqueous solution at 60°C–85°C for 40 minutes. The experiment was repeated three times, and the results were averaged with standard deviation.

Statistical analysis

The cell multiplying experiment was conducted in triplicate and the results are presented as means ± standard deviations. The Student's *t*-test was used to estimate the statistically significant difference between the results. Difference was considered statistically significant at $P<0.05$.

Discussion

Surface characterization

The surface modification of GNP with herceptin was confirmed by UV–vis spectra, as shown in Figure 2. GNPs showed an absorption onset at 386 nm and after herceptin immobilization, they exhibited a red shift to 389 nm.[26] This red shift was produced by strong quantum confinement due to the increase in particle size after metal-to-ligand charge transfer.[27,28] The surface modification of GNP with herceptin was also confirmed by FT-IR, as displayed in Figure 3. In the case of the GNP spectrum, the introduction of MSA on the surface of GNP was confirmed by the characteristic peak at 1,700 cm^{-1} and 3,500 cm^{-1} (Figure 3A), which can be attributed to the free carboxyl (—COOH) and hydroxyl (—OH) groups.[26,29] Again, after reaction of GNP with herceptin, two new peaks at positions around 1,648 cm^{-1} and 1,540 cm^{-1} were observed in the spectrum of GNP–Her (Figure 3B), which are assigned to the amide I (—CO—NH—) and amide II (—CO—NH—) bonds,

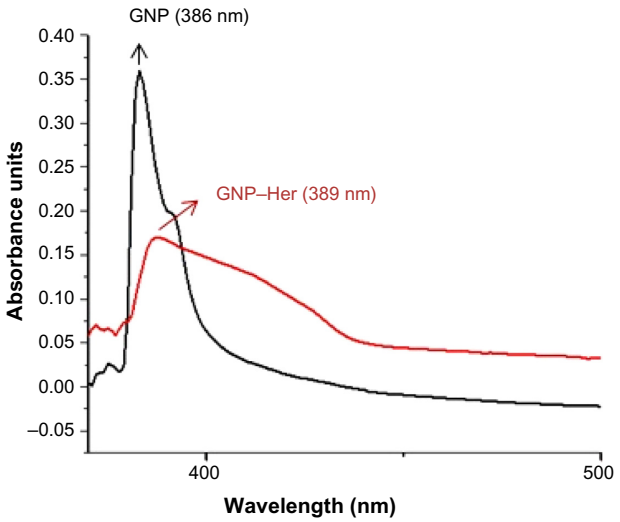

Figure 2 UV spectra of GNP and GNP–Her.
Abbreviations: GNP, gold nanoparticle; GNP–Her, herceptin-conjugated GNP; UV, ultraviolet.

respectively.[29] After the reaction of the free amine groups of GNP with herceptin, absorption at 1,648 cm^{-1} and 1,540 cm^{-1} appeared, due to the amide groups of GNP–Her, proving the effective immobilization of herceptin over the GNPs.

Figure 4 represents the TEM images of GNP and GNP–Her. The GNP has a spherical morphology, with a mean diameter of ~7.34 nm. In the case of GNP–Her, the particles had a mean diameter of ~8.14 nm, were spherical in shape, and showed significantly monodispersed particles (Figure 4B). The larger particle size and nonaggregated particle morphology was attributed to the conjugation of herceptin on the surface of the GNP. Figure 5 shows the typical sizes and size distributions of the synthesized GNPs and GNP–Her conjugates measured by DLS. The mean size of the GNPs, as determined by DLS, was ~29 nm. On the other hand, the mean size of GNP–Her was almost ~82 nm. The particle size, as determined by DLS, was significantly larger than that determined by TEM. This is because the DLS technique measures the mean hydrodynamic diameter of the GNP core bounded by the organic and solvation layers, and this hydrodynamic diameter is affected by the viscosity and concentration of the medium. TEM, however, gives the diameter of the core alone.[27] The synthesis of Cy5 dye-immobilized GNP–Her was also confirmed by UV–vis absorption spectroscopy, as shown in Figure 6. The Cy5 dye-immobilized GNP–Her showed an absorption onset at 263 nm (Figure 6B) and after Cy5 dye immobilization, it exhibited a red shift to 680 nm (Figure 6A). This red shift was caused due to the increase in particle diameter.[28]

Evaluation of cytotoxicity

Figure 7 shows the distinction of the "live/dead" dye-stained SK-BR3 and FB cells cultured in the presence of GNP and GNP–Her after 3 days of incubation. Using this qualitative method, the living and the dead cells were stained green and red, respectively, and were visible by fluorescence microscopy. Figure 7A shows that all the FB cells remained viable after 3 days' incubation, in the presence of NPs. On the other hand, after culturing for 3 days, in the presence of GNP–Her, most of the SK-BR3 cells had died, as shown in Figure 7B. Figure 8 shows the viability of SK-BR3 cells cultured for 1 day and 3 days in the presence of GNP–Her, as determined by the MTT (3-(4,5-dimethylthiazol-2-yl)-2,5-diphenyltetrazolium bromide)assay. After 1 day and 3 days of incubation, the level of SK-BR3 cell proliferation in the presence of GNP was similar to that of the cells cultured in the absence of NPs (polystyrene dish). On the other hand, cell propagation in the presence of GNP–Her was significantly lower than that in the

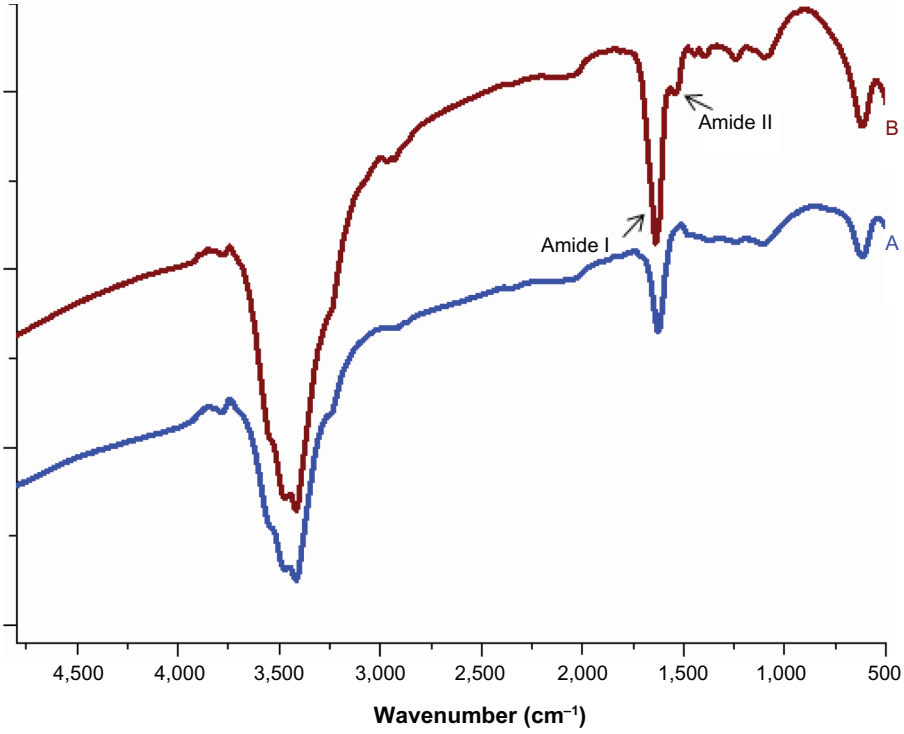

Figure 3 FT-IR spectra of GNP (**A**) and GNP–Her (**B**) measured using the KBr method.
Abbreviations: FT-IR, Fourier transform infrared; GNP, gold nanoparticle; GNP–Her, herceptin-conjugated GNP; KBr, potassium bromide.

presence of GNP. Therefore, the GNP conjugated with herceptin could increase the death of SK-BR3 cells considerably compared to the GNP without herceptin.

A probable explanation of this large decrease in cell viability in the case of GNP–Her is that intracellularly distributed herceptin shows significant apoptotic activity by networking with several transcription factors related to cell propagation. Formerly, Bae et al[30] stated that degradable heparin nanogels and heparin/chitosan polyelectrolyte nanocomplexes could effectively induce apoptosis via receptor-mediated endocytosis through specific herceptin–HER2–integrin interaction. The endocytosed GNP–Her within the cells discharge free herceptin molecules in the cytoplasm by slicing the GNP–herceptin linkage under the reductive intracellular environment, which has a 300 times greater glutathione concentration than extracellular medium.[28] Glutathione is the main abundant reducing agent in the cytoplasm, helping in the dissipation of herceptin from the GNP by breaking the MSA–herceptin linkage. Furthermore, NPs are taken up by the cells through endocytosis, which disrupts the cell membrane, or weak cell adhesive interactions

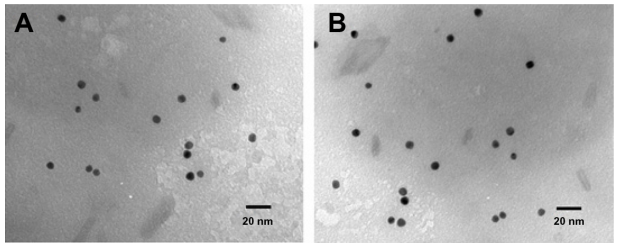

Figure 4 TEM images of GNP (**A**) and GNP–Her (**B**).
Abbreviations: TEM, transmission electron microscopy; GNP, gold nanoparticle; GNP–Her, herceptin-conjugated GNP.

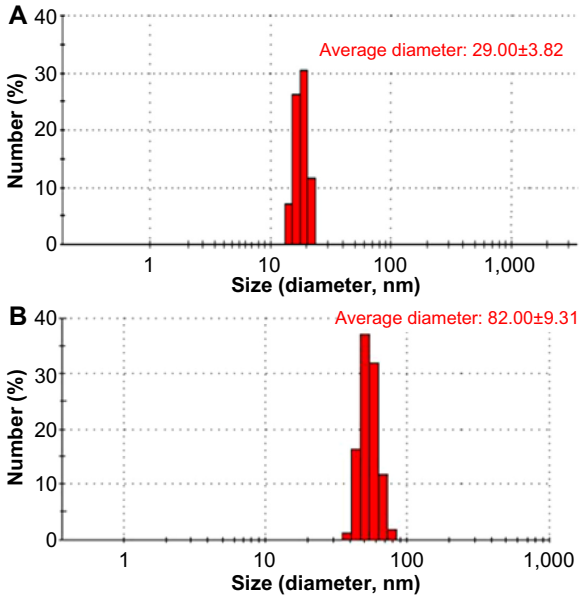

Figure 5 Particle-size distributions of GNP (**A**) and GNP–Her (**B**) measured by DLS.
Abbreviations: DLS, dynamic light scattering; GNP, gold nanoparticle; GNP–Her, herceptin-conjugated GNP.

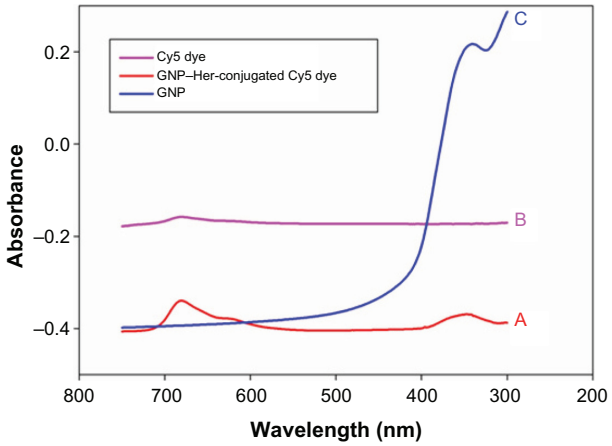

Figure 6 UV–vis absorption spectra of the GNP–Her-conjugated Cy5 dye (**A**), Cy5 dye (**B**), and GNP (**C**) in aqueous solution.
Abbreviations: GNP, gold nanoparticle; GNP–Her, herceptin-conjugated GNP; UV–vis, ultraviolet–visible.

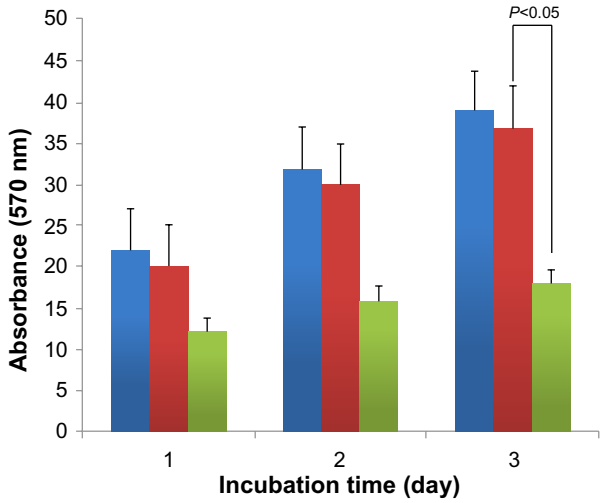

Figure 8 MTT assay.
Notes: Absorbance as a measure of the cell proliferation of SK-BR3 cells cultured in the polystyrene culture dish (the blue bar), in the presence of GNP (the red bar), and with GNP–Her (the green bar) for different time periods.
Abbreviations: GNP, gold nanoparticle; GNP–Her, herceptin-conjugated GNP; MTT, 3-(4,5-dimethylthiazol-2-yl)-2,5-diphenyltetrazolium bromide.

with GNP may encourage apoptosis. GNPs conjugated with herceptin may act as cellular markers and target the receptors expressed on the cell exterior, with cellular internalization.[31] The receptors are highly controlled by the cell surface proteins, which facilitate the specific communication between cells and their extracellular environments, and they are usually confined on the plasma membrane.[32]

Estimation of intracellular uptake

The quantity of GNP–Her taken up by SK-BR3 cells was estimated by ICP–MS and the outcomes are presented in Figure 9. After herceptin conjugation, the NPs' interaction with SK-BR cells was amplified significantly, in contrast to that of the original NPs, and increased to 1.4 pg per cell within the first day of culture, much higher than that of the original NPs.[33] The peak internalization of GNP–Her occurred at 4.6 pg per cell after 3 days of culture. The cause for the uptake enhancement might be ligand–receptor interactions on the cell membrane.[34] Moreover, the greater uptake of herceptin-modified GNPs indicates that the alteration not only enabled the NPs to target specific cells but also improved the cell internalization yield. Similar results obtained from (carboxymethyl)chitosan-modified superparamagnetic iron oxide nanoparticles were shown by Shi et al[35] in their reports; the quantity of NPs internalized in human muscle-derived cells is much more than that of superparamagnetic iron oxide nanoparticles, as observed by ICP–MS. The interaction between herceptin and SK-BR3

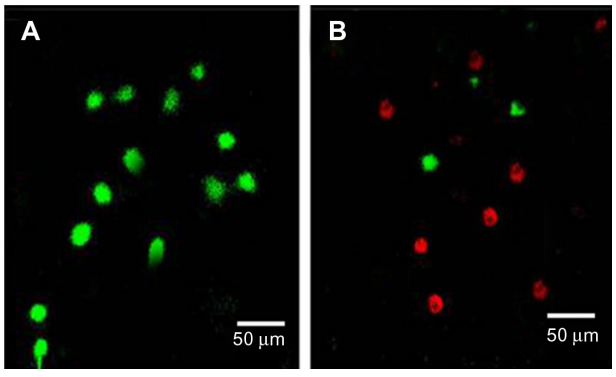

Figure 7 Fluorescence microscopy.
Notes: Fluorescence microscopy images of live and dead FB (**A**) and SK-BR3 (**B**) cells after culturing for 3 days in a polystyrene culture dish in the presence of culture medium and GNP–Her. The live and dead cells were stained and visualized in green and red, respectively, under a fluorescence microscope.
Abbreviations: GNP, gold nanoparticle; GNP–Her, herceptin-conjugated GNP; FB, fibroblast cell line.

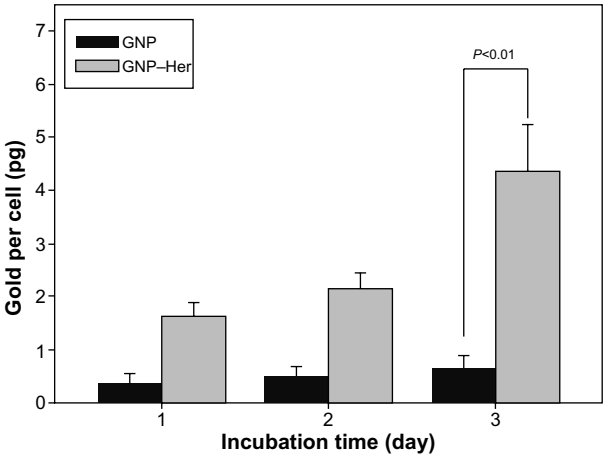

Figure 9 Amount of GNP (black bar) and GNP–Her (gray bar) taken up by SK-BR3 cells at different incubation times, as determined by ICP–MS.
Abbreviations: GNP, gold nanoparticle; GNP–Her, herceptin-conjugated GNP; ICP–MS, inductively coupled plasma mass spectrometry.

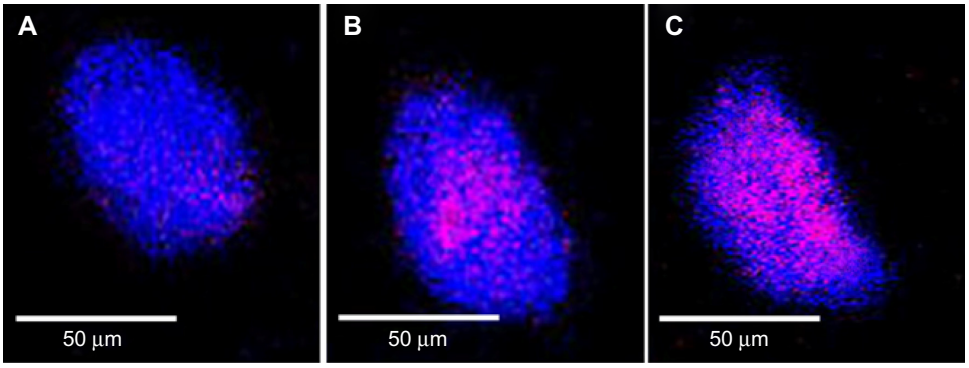

Figure 10 Fluorescence images of SK-BR3 cells.
Notes: Images were obtained from the culture of SK-BR3 cells for 1 hour (**A**), 3 hours (**B**), and 6 hours (**C**) in the presence of DAPI, and these show specific HER2 interaction with herceptin.
Abbreviations: HER2, human epidermal growth factor receptor 2; DAPI, 4,6-diamidino-2-phenylindole dihydrochloride.

receptors expressed on the membrane might have contributed to the enhancement of GNP–Her internalization based on receptor-mediated endocytosis.[36]

The internalization of GNP–Her into SK-BR3 cells was also confirmed by CLSM. Figure 10 shows that herceptin is an effective antibody, binding specifically to the HER2-bearing breast tumor cells. The internalization of GNP–Her into SK-BR3 cells was confirmed by CLSM to characterize the delivery of GNP–Her to the cytoplasm of the SK-BR3 cells. The fluorescence image was derived from the nucleus of the SK-BR3 cells (DAPI, blue) and the internalized GNP–Her (red). The cells were cultured in the presence of GNP–Her at various incubation times. Weak GNP–Her conjugates were observed in the fluorescence image (red color) after 1 hour (Figure 10A) and slightly higher fluorescence was observed after 3 hours (Figure 10B). Intense fluorescence was noted after 6 hours (Figure 10C). On the other hand, the blue fluorescence derived from the nuclei stained with DAPI was strong after 1 hour of incubation, but it decreased with increasing incubation time and almost disappeared after 6 hours of incubation. In particular, the interaction of SK-BR3 with GNP–Her began after 1 hour of incubation and was accelerated and saturated after 6 hours. The CLSM images suggest that the NP-mediated delivery of monoclonal antibodies was achieved efficiently, resulting in cell death.[36] The mechanism of internalization involves endocytosis, followed by the release of herceptin-conjugated NPs to the cytoplasm.[29,37] This suggests that the growth signal of SK-BR3 cells is withdrawn completely by the specific binding of herceptin to the receptor on SK-BR3 membrane, resulting in cell death.[35,36]

Conclusion

MSA-coated GNP was conjugated successfully with herceptin, which was confirmed by UV–vis and FT-IR spectroscopy techniques. The size of GNP determined by DLS was ~79 nm, whereas that of the GNP–Her was ~86 nm. GNP–Her had no cytotoxic effect on the control cells (FB) compared to the target cells (SK-BR3) and was internalized selectively into the target cells (SK-BR3); the free herceptin was delivered into the cytoplasm, which induced acute apoptosis. The GNP–Her NPs underwent endocytosis in breast cancer cells (SK-BR3) largely through a receptor-facilitated mechanism, whereby herceptin conjugated on the NPs targets the HER2 expressed on the membrane of the cancer cells.[29] Therefore, GNP–Her has potential use in the optical imaging and treatment of breast cancer.

Acknowledgments

This work was supported by Institute of Biomedical Technologies, Auckland University of Technology, New Zealand. Dr Huh is grateful for the grant supported from the Research Foundation of Korea (NRF-2013R1A1A2A100062399) for technical support in cell culturing experiments.

Disclosure

The authors report no conflicts of interest in this work.

References

1. David ME, Choi CH, Seligson DA, Tolcher A, Dordick JS, Alabi CA. Evidence of RNAi in humans from systemically administered siRNA via targeted nanoparticles. *Nature*. 2010;464:1067–1070.
2. Han G, You CC, Kim BJ, Forbes R, Turingan RS, Martin CT. Light-regulated release of DNA and its delivery to nuclei by means of photolabile gold nanoparticles. *Angew Chem Int Ed*. 2006;45(19):3165–3169.
3. El-Sayed IH, Huang X, El-Sayed MA, Tolcher A, Dordick JS, Alabi CA. Selective laser photo-thermal therapy of epithelial carcinoma using anti-ER antibody conjugated gold nanoparticles. *Cancer Lett*. 2006;239(1):129–135.
4. Allen TM. Ligand-targeted therapeutics in anticancer therapy. *Angew Chem Int Ed*. 2002;2(10):705–763.
5. Chaterjee DK, Rufalhah AJ, Zhang Y, Tolcher A. Upconversion fluorescence imaging of cells and small animals using lanthanide doped nanocrystals. *Biomaterials*. 2008;29(7):937–943.

6. Wang CS. Gold nanoclusters and graphene nanocomposites for drug delivery and imaging of cancer cells. *Angew Chem Int Ed*. 2011;50:11644–11648.
7. Pan J, Feng SS. Targeting and imaging cancer cells by folate-decorated, quantum dots (QDs) – loaded nanoparticles of biodegradable polymers. *Biomaterials*. 2009;30:1176–1183.
8. Jiang S, Gnanasammandhan MK, Zhang Y. Optical imaging-guided cancer therapy with fluorescent. *J R Soc Interface*. 2010;7(1):3–18.
9. Román-Velázquez CE, Noguez C, Garzón IL. Circular dichroism simulated spectra of chiral gold nanoclusters: a dipole approximation. *J Phys Chem B*. 2003;107(44):12035–12038.
10. Peyser LA, Vinson AE, Bartko AP, Dickson RM. Photoactivated fluorescence from individual silver nanoclusters. *Science*. 2001;291(5501):103–106.
11. Yang Y, Chen S. Surface manipulation of the electronic energy of Sub nanometer-sized gold clusters: an electrochemical and spectroscopic investigation. *Nano Lett*. 2003;3(1):75–79.
12. Zheng J, Dickson RM. Individual water-soluble dendrimer-encapsulated silver nanodot fluorescence. *J Am Chem Soc*. 2002;124(47):13982–13983.
13. Hvkkinen H. Electronic, and impurity-doping effects in nanoscale chemistry: supported gold nanoclusters. *Angew Chem Int Ed*. 2003;42(11):1297–1300.
14. Crespo P. Permanent magnetism, magnetic anisotropy, and hysteresis of Thiol-capped gold nanoparticles. *Phys Rev Lett*. 2004;93(1):872041–872044.
15. Balaban RS, Nemoto S, Finkel T. Mitochondria oxidants and aging. *Cell*. 2005;120(1):483–495.
16. Lim CK. Chemiluminescence-generating nanoreactor formulation for near-infrared imaging of hydrogen peroxide and glucose level in vivo. *Adv Funct Mater*. 2010;20(16):2644–2648.
17. Mannervik B. The enzymes of glutathione metabolism: an overview. *Biochem Soc Trans*. 1987;15(4):717–718.
18. Scott D, Toney M, Muzikar M. Harnessing the mechanism of glutathione reductase for synthesis of active site bound metallic nanoparticles and electrical connection to electrodes. *J Am Chem Soc*. 2008;130(3):865–874.
19. McCarthy JR, Bhaumik J, Karver MR, Sibel Erdem S, Weissleder R. Targeted nanoagents for the detection of cancers. *Mol Oncol*. 2010;4(6):511–528.
20. Lee JF, Stovall GNP, Ellington AD. Aptamer therapeutics advance. *Curr Opin Chem Biol*. 2006;10(3):282–289.
21. Lu W, Zhang G, Zhang R, Flores LG, Huang Q, Gelovani JG. Tumor site-specific silencing of NF-kappaB p65 by targeted hollow gold nanosphere-mediated photothermal transfection. *Cancer Res*. 2010;70(8):3177–3188.
22. Karin M, Cao Y, Greten FR, Li ZW. NF-κB in cancer: from innocent by stander to major culprit. *Nat Rev Cancer*. 2002;2(4):301–310.
23. Lee CM, Jeong HJ, Kim EM, Kim DW, Lim ST, Kim HT. Superparamagnetic iron oxide nanoparticles as a dual imaging probe for targeting hepatocytes in vivo. *Magn Reson Imaging*. 2009;62(6):1440–1446.
24. Anshup A, Venkatraaman JS, Chandramouli S, Pradeep T. Growth of gold nanoparticles in human cells. *Langmuir*. 2005;21(25):11562–11567.
25. Ogawa M, Regino CAS, Choyke PT. In vivo target-specific activatable near-infrared optical labeling of humanized monoclonal antibodies. *Mol Cancer Ther*. 2009;8:232–239.
26. Xing ZC, Park MJ, Han SJ, Choi MJ, Lee BH, Kang IK. Intracellular Uptake of magnetite nanoparticles conjugated with RGDS-peptide. *Macromol Res*. 2011;19(9):897–903.
27. Lee YK, Hong SM, Kim JS, Im JH, Park SW. Encapsulation of CdSe/Zns quantum dots in poly(ethyleneglycol)-poly(D,L-lactide) micelle for biomedical imaging and detection. *Macromol Res*. 2007;15(4):330–336.
28. Kamuruzzaman Selim KM, Xing ZC, Choi MJ, Chang Y, Guo H, Kang IK. Reduced cytotoxicity of insulin-immobilized CdS quantum dots using PEG as a spacer. *Nanoscale Res Lett*. 2011;6(1):528–536.
29. Li J, Jiang F, Yang B, Song XR, Li Y, Yang H. Topological insulator bismuth selenide as a theranostic platform for simultaneous cancer imaging and therapy. *Sci Rep*. 2013;3(1):1–7.
30. Bae KH, Mok H, Park T. Synthesis characterization, and intracellular delivery of reducible heparin nanogels for apoptotic cell death. *Biomaterials*. 2008;29(23):3376–3383.
31. Koo T, Borah JS, Xing ZC, Kang IK. Immobilization of pamidronic acids on the nanotube surface of titanium discs and their interaction with bone cells. *Nanoscale Res Lett*. 2013;8(1):124–133.
32. Gan J, Jiang S, Yang Y. Immobilization of homing peptide on magnetite nanoparticles and its specificity in vitro. *J Bio Med Mater Res Part A*. 2008;27(1):468–476.
33. Hong R, Han G, Fernandez J, Kim MB, Forbes NS, Rotello VM. Glutathione-mediated delivery and release using monolayer protected nanoparticle carriers. *J Am Chem Soc*. 2006;128(4):1078–1089.
34. Gomes PF, Godoy MPF, Veloso AB, Madhireira JR. Exciton binding energy in type II quantum dots. *Phys Status Solidi*. 2007;4(2):385–388.
35. Shi Z, Neoh KG, Kang ET, Wang SC, Wang W. Carboxymethyl chitosan-modified super magnetic iron oxide nanoparticles for magnetic resonance imaging of stem cells. *ACS Appl Mater Interfaces*. 2009;1:328–335.
36. Han SJ, Pierson R, Kang IK. Specific intracellular uptake of herceptin-conjugated CdSe/ZnS quantum dots into breast cancer cells. *Bio-Med Res Int*. 2014;14:954307–954309.
37. Geelen T, Nicoloy K, Paulis LM, Yeo SY, Strijkers GJ. Internalization of paramagnetic phosphatidylserine-containing liposomes by macrophages. *J Biotechnol*. 2012;10(37):1–11.
38. Yamaura M, Camilo RL, Sampaio LC. Preparation and characterization of (3aminopropyl) triethosysilane-coated magnetite nanoparticles. *J Magn Magn Mater*. 2004;1:210–217.
39. Bale SS, Kwon SJ, Shah DA, Banerjee A, Dordick JS, Kane RS. Nanoparticle-mediated cytoplasmic delivery of proteins to target cellular machinery. *J Am Chem Soc*. 2010;4(3):1493–1500.